

WHAT WE ALREADY KNOW ABOUT QUINTESSENCE

Sidney Bludman*

Deutsches Elektronen-Synchrotron DESY, Hamburg

University of Pennsylvania, Philadelphia

(Dated: February 2, 2008)

Good tracking requires significant quintessence energy fraction, even in the past, but a potential energy that is not yet truly slow-rolling. The supernova bound on cosmic acceleration excludes constant equation of state and inverse power potentials, but allows the SUGRA potential and other good trackers, in which quintessence energy domination and kinetic energy suppression *both* began only recently. This makes the time in which we live special in *two* respects.

I. THE DARK ENERGY DENSITY IS NOW EXACTLY OR NEARLY STATIC

A. Kinematics of the Expanding and Accelerating Universe

Supernovae Ia, cosmic shear, and angular diameter measurements all directly explore the space-time geometry by measuring the luminosity distance $d_L(z) = (1+z)\eta$ or the angular-diameter distance $d_A(z) = \eta/(1+z)$, from which the comoving distance

$$\eta \equiv c \int_0^z dz'/H(z') = c \int_0^t dt'/a(t') \quad (1)$$

to individual distant supernovae, chosen to be standard candles, or to distant galaxies is inferred. (The conformal coordinate distance to the horizon, η , describes the proper time evolution of the scale factor a .) Assuming a homogeneous and isotropic (Robertson-Walker) flat universe, the Friedmann expansion rate is

$$8\pi G\rho = 3H^2, \quad \text{where} \quad H \equiv \dot{a}/a. \quad (2)$$

Quantum field theory requires that the energy density, and therefore G , be positive, so that we can write $\sqrt{8\pi G} \equiv \kappa \equiv 1/M_P$, where $M_P = 2.44e18 \text{ GeV}$ is the reduced Planck mass. The derived quantity, the cosmological fluid pressure $P = -d(\rho c^2 a^3)/da^3$, may be positive or negative.

In terms of geometrical quantities,

$$\kappa^2 P/c^2 = -(2\dot{H} + 3H^2), \quad (3)$$

the enthalpy is

$$\kappa^2(\rho + P/c^2) = -2\dot{H} = -dH^2/dN = -(\kappa^2/3)(d\rho/dN), \quad (4)$$

and the over-all barotropic index is

$$\gamma \equiv -d \ln \rho / 3dN = (\rho + P/c^2)/\rho = -\frac{2}{3}(d \ln H / dN). \quad (5)$$

Here the logarithm of the cosmological scale factor $N \equiv \ln a = -\ln(1+z)$, so that $dN = Hdt$. This equation of state and its quintessence component do not depend on the Hubble radius H^{-1} , but on its derivative i.e. not on the comoving distance η , but on $d\eta/dz$, $d^2\eta/dz^2$. In cosmologies satisfying the Weak Energy Condition $\rho + P/c^2 > 0$, $\dot{H} < 0$, so that the expansion is monotonic. We will not consider alternate gravity theories, such as extra dimensions, in which the Friedmann equation (2) is modified.

In cosmology, the Ricci scalar is

$$R \equiv -6(\dot{H} + 2H^2) = -\kappa^2(\rho - 3P), \quad (6)$$

*bludman@mail.desy.de

while the acceleration, $\ddot{a}/a = -\kappa^2(\rho + 3P)/6$, so that

$$\ddot{a}/\dot{a}^2 = 1 - d(H^{-1})/dt = -(1 + 3w)/2 \quad (7)$$

ranges from -2 to 1 , when the overall equation of state $w \equiv P/\rho$ ranges from 1 to -1 . We now know that, until about red-shift $z \sim 0.7$, attractive gravity dominated the cosmological fluid so that large scale structures could form. Only recently, after the expansion rate in equation (7) outpaced the growth of the Hubble radius H^{-1} , did $P/\rho = w_Q \Omega_Q < -1/3$, and the expansion become accelerated. Interestingly, this direct observation of acceleration in the present universe supports the possibility of an inflationary early universe, which is otherwise not directly observable.

Because the barotropic index (5) and its quintessence component (13) depend on the first and second derivatives of the comoving distance η , the quintessence evolution $w_Q(z)$ depends on first and second derivatives of the observed luminosity distances [1]. In practice, quintessence is appreciable only for small red-shift. This means that, before $w_Q(z)$ can be determined, the inherently noisy luminosity distance $d_L(z)$ data must be parametrized. For this, and other reasons, along with a large number of high red-shift supernovae, precise knowledge of other cosmological parameters will be needed [2, 3, 35], and can still determine only one or two parameters characterizing the potential, such as w_{Q0} , $(dw_Q/dz)_0$.

While programs to measure luminosity and angular diameter distances are underway, we already know that we live at a time when

$$\Omega_{Q0} = 0.71 \pm 0.07, \quad \widetilde{w}_Q < -0.78 \text{ (95\% CL)}, \quad h \equiv H_0/100 = 0.72 \pm 0.05, \quad (8)$$

that the radiation/matter equality took place at red-shift $z_{eq} = 3454^{+385}_{-392}$ [5, 6, 7, 8, 9, 10, 11, 12], dark energy began dominating over matter $\gtrsim 6.3 \text{ Gyr}$ ago, and the cosmological expansion has been accelerating since red-shift $z \sim 0.7$ [4, 6]. The background density,

$$\rho_B = (11.67a + 0.003378)/a^4 \quad \text{meV}^4, \quad (9)$$

is now $\rho_{B0} = 11.67 \text{ meV}^4$ and was $\rho_{Bi} = 0.003378 \text{ GeV}^4$ at fiducial red-shift $z = 10^{12}$. The supernova observations fit an average

$$\widetilde{w}_Q(N) \equiv \int_0^N w_Q(N') dN'/N,$$

over a small range in z , in which the quintessence field and $w_Q(z)$ change relatively little, so that an approximate bound on w_{Q0} is the fitted $\widetilde{w}_Q < -0.78$. The CBR anisotropy and mass fluctuation spectrum, on the other hand, depend on "early quintessence" [13], back to the last scattering surface $z \sim 1100$. Where needed, we will fix $h^2 = 1/2$, so that the present critical density and smooth energy density are $\rho_{cr0} = 40.5 \text{ meV}^4$, $\rho_{Q0} = 28.8 \text{ meV}^4$.

We will show that these observational constraints (8) allow only crawling quintessence (Section III) or potentials with large current curvature (Section IV), "cross-over quintessence" [15]. We go beyond the many earlier optimistic treatments of the Attractor Condition [14, 16, 17, 18, 19, 20, 21] and of inverse power potentials [22, 23], to consider (1) poor trackers, (2) post-tracker behavior in the present quintessence-dominated era, (3) the range of initial conditions that would lead to tracking, and (4) the numerical problems encountered in cosmological dynamics, particularly in the freezing and tracking epochs. But first we will review (Section II) the Attractor Condition, in order to show how the basin of attraction shrinks for potentials satisfying the observational constraints (8).

B. Quintessence Dynamics: Potentials Not Yet Truly Slow-Rolling

The universe is flat, presently dominated by smooth energy, and recently accelerated. Canonical quintessence models the smooth energy dynamically by a spatially homogeneous light classical scalar field, with canonical kinetic energy $K = \dot{\phi}^2/2$, minimal gravitational coupling, zero true cosmological constant, rolling down its self-potential $V(\phi)$. This quintessence field generically has good-or-bad attractor properties [22, 23], making the present universe more-or-less insensitive to a broad range initial conditions. Tracking quintessence was invoked to use this attractor property to explain the small cosmological constant or present smooth energy density, without fine tuning of the potential or initial conditions. In canonical quintessence, the scalar field equation of motion

$$\ddot{\phi} + 3H\dot{\phi} + dV/d\phi = 0, \quad (10)$$

has the first integral

$$V(N) = \rho_Q + d\rho_Q/6dN = \rho_Q(1 - w_Q)/2, \quad (11)$$

where the energy density and pressure are

$$\rho_Q = \dot{\phi}^2/2 + V(\phi), \quad P/c^2 = \dot{\phi}^2/2 - V(\phi), \quad (12)$$

and the quintessence barotropic index

$$\gamma_Q(N) \equiv -d \ln \rho_Q / 3dN = ((\rho + P/c^2)/\rho)_Q \equiv 1 + w_Q \quad (13)$$

lies between 0 and 2. Because the scalar field does not cluster on supercluster scales, its mass must be $\lesssim 10^{-31} eV$, which is incredibly small.

From the energy integral (12), $\dot{\phi}^2 = \gamma_Q \rho_Q$ or $(\kappa d\phi/dN)^2 = 6x^2$, where $x^2 \equiv \dot{\phi}^2/2\rho = \gamma_Q \Omega_Q/2$ is the quintessence kinetic energy fraction of the total energy density. The ratio of kinetic/potential energy $K/V = (1 + w_Q)/(1 - w_Q)$ has the rate of change $d \ln(K/V)/dN = 6(\Delta - 1)$, where $\Delta(N) \equiv -d \ln V/3\gamma_Q dN$. Thus, the *roll*,

$$\lambda \equiv -d \ln V / \kappa d\phi = \sqrt{3\gamma_Q/\Omega_Q} \cdot \Delta, \quad (14)$$

and

$$dw_Q/dN = 3(1 - w_Q^2)(\Delta - 1), \quad \kappa d\phi/dN = \sqrt{3\gamma_Q\Omega_Q} \quad (15)$$

is a two-element non-autonomous system for the dependent variables ϕ , w_Q . Integrating the second equation (15) implicitly relates ϕ and $V(\phi)$, so that, if the equation of state $w_Q(N)$ can be observed, the potential can be reconstructed. The overall equation of state is

$$w = \gamma - 1 = w_B \Omega_B + w_Q \Omega_Q, \quad (16)$$

where the dimensionless ratios, Ω_Q , $\Omega_B \equiv \rho_B/(\rho + \rho_Q)$, are the energy density fractions in quintessence and in the background, and γ_Q , $\gamma_B \equiv -d \ln \rho_B/3dN$ are their corresponding barotropic indices. Defining the potential energy fraction $y(N)^2 \equiv V_Q/\rho$, equations (15) have scaling solutions, when $\gamma_Q \approx \text{const}$: kination, when $\gamma_Q = 2, x \gg y$; freezing, when $\gamma_Q = 0, x \ll y$; tracking, when $\gamma_Q = \gamma_B\beta/(\beta + 2)$ and $(y/x)^2 \equiv V/K = 2/\gamma_Q - 1 \approx \text{const}$.

Besides the roll λ , the potential depends on the curvature $\eta \equiv d^2V/V(\kappa d\phi)^2$. When the roll is flat ($\epsilon \equiv \lambda^2/2 \ll 1$), the kinetic energy $\dot{\phi}^2/2$ is negligible in the quintessence energy (12). When the curvature is small ($\eta \ll 1$, $\ddot{\phi}$ is negligible in the equation of motion (10)). In ordinary inflation, both these conditions hold (*slow roll approximation*): the expansion is dominated by the cosmological drag and the field is nearly frozen. But, in quintessence, the acceleration began only recently, so that the roll λ_0 and curvature η_0 are still $\mathcal{O}(1)$. This invalidates the slow roll approximation for quintessence, so that the dynamical equations need to be integrated numerically. We ultimately handled the kination/freezing and freezing/tracking transitions and numerical stability and round-off problems in the protracted frozen era, by implicit Adams backward differentiation procedures (Maple lode[adamsfunc] and lode[backfull]), with small adaptive step-size.

Unless it undergoes a first-order phase transition, the quintessence field rolls monotonically towards a minimum at $\phi = \infty$ or at some finite ϕ_{\min} : either way, the potentials we consider are always convex. (Presumably, there is no true cosmological constant so that the potential energy vanishes asymptotically, avoiding the possibly worrisome future de Sitter event horizon, with attendant diminution of causal connectivity in the far future.) Defining $\Gamma \equiv V d^2V/d\phi^2/(dV/d\phi)^2$, so that $\eta = \lambda^2\Gamma$, we have $1/\beta(\phi) \equiv \Gamma - 1 = \lambda^2 d^2 \ln V / \kappa^2 d\phi^2 = d(1/\lambda)/\kappa d\phi > 0$.

Both the roll and the curvature, λ , β are listed in Table I, for five different potentials. The first, third and fourth rows in Table I list three potentials with constant inverse curvature $1/\beta$: the cosmological constant, inverse power, and exponential, for $\beta = 0, \text{const} \equiv \alpha, \infty$ respectively. On the second row, where $\tilde{\alpha} \equiv \sqrt{\gamma_Q}/\alpha$, the *constant w_Q model* interpolates between the inverse power potential, when $\tilde{\alpha}\kappa\phi \ll 1$, and the exponential when $\tilde{\alpha}\kappa\phi \gg 1$. The bottom row in Table I is the more realistic inflaton broken-SUSY SUGRA potential, in which $\beta(\phi)$ decreases significantly for $\phi \gtrsim M_P$.

C. Phaseportrait in Terms of Quintessence Kinetic, Potential Energy Canonical Variables

In place of the phase variables ϕ , $w_Q \equiv (P/\rho)_Q$, we may use $x \equiv (\kappa d\phi/dN)/\sqrt{6}$, $y \equiv \sqrt{V/\rho}$, for which the equations of motion are [18, 19, 20, 21]

$$dx/dN = -3x + \lambda\sqrt{3/2}y^2 + 3x\gamma/2 \quad (17)$$

$$dy/dN = -\lambda\sqrt{3/2}xy + 3y\gamma/2 \quad (18)$$

$$d\lambda/dN = -\sqrt{6}\lambda^2x/\beta \quad \text{or} \quad d(1/\lambda)/dN = \sqrt{6}x/\beta. \quad (19)$$

TABLE I: Potentials described by roll $\lambda = -d \ln V / \kappa d\phi$ and curvature $\eta = d^2 V / V d(\kappa\phi)^2$.

$V(\phi)$	$\lambda(\phi)$	$\eta(\phi) = \lambda^2 \Gamma$	$\Gamma - 1 = 1/\beta(\phi)$	NAME
$\exp -\lambda \kappa \phi$	$\lambda = \text{const} > \sqrt{3\gamma_B}$	$\lambda^2 = \text{const} > 3\gamma_B$	0	exponential
$1/\sinh^\alpha(\tilde{\alpha}\kappa\phi)$	$(\alpha\tilde{\alpha}) \coth(\tilde{\alpha}\kappa\phi)$	$(\alpha\tilde{\alpha})^2[(1+\alpha)\coth(\tilde{\alpha}\kappa\phi) - 1]$	$1/\alpha \cosh^2(\tilde{\alpha}\kappa\phi)$	const $w_Q = -2/(2+\alpha)$
$\phi^{-\alpha}$	$\alpha/\kappa\phi$	$\alpha(\alpha+1)/(\kappa\phi)^2$	$1/\alpha$	inverse power
const	0	0	∞	cosmological const
$\phi^{-\alpha} \cdot \exp \frac{1}{2}(\kappa\phi)^2$	$\alpha/\kappa\phi - \kappa\phi$	$[\alpha(\alpha+1) - \alpha(\kappa\phi)^2 + (\kappa\phi)^4]/(\kappa\phi)^2$	$(\alpha + (\kappa\phi)^2)/(\alpha - (\kappa\phi)^2)^2$	SUGRA

The overall equation of state of our two-component mixture of background and quintessence, $\gamma = \gamma_Q \Omega_Q + \gamma_B \Omega_B = 2x^2 + \gamma_B(1 - x^2 - y^2)$, is a time-dependent function of the scalar field $\phi(N)$. Thus,

$$x^2 + y^2 = \Omega_Q, \quad 2x^2 = \Omega_Q \gamma_Q, \quad y^2/x^2 = V/K = (1 - w_Q)/(1 + w_Q), \quad d \ln(x^2/y^2)/dN = 6(\Delta - 1). \quad (20)$$

The three-element system (17-19) is autonomous, except for the slow change in $\gamma_B(N)$ from 4/3 to 1, while gradually going from the radiation-dominated to the matter-dominated universe, around red-shift $z_{eq} = 3454$.

The magnitude of V needs to be fitted to the present value $V_0 = \rho_{cr0} y_0^2 = \rho_{Q0}(1 - w_{Q0})/2$. For example, inverse power potentials, require energy scale $M_\alpha = (V_0 \phi_0^\alpha)^{1/(4+\alpha)}$, listed in the fourth column of Table II. For shallow potentials ($\alpha < 0.2$), this energy scale is close to observed neutrino masses and to the present radiation temperature, possibly suggesting some role for the neutrino mass mechanism or for the matter/radiation transition, in bringing about quintessence dominance. For steep potentials ($\alpha > 1$), this mass scale can be considerably larger, suggesting the larger scales we encounter in particle physics.

While the evolution of a homogeneous scalar field depends only on its equation of state $w_Q = (P/\rho c^2)_Q$, the growth of its fluctuations depends also on the quintessence sound speed $c_s^2 = (dP/d\phi)/(d\rho_Q/d\phi)$. With the linear form for the kinetic energy $K = \dot{\phi}^2/2$ that canonical quintessence assumes, $c_s^2 = c^2$ and $-1 \leq w_Q \leq 1$, $dw_Q/dz > 0$. Non-canonical forms, as in k-essence [24, 25], would allow $w_Q < -1$, $dw_Q(z)/dz < 0$ and give different sound speed and structure evolution. Despite this difference in sign of dw_Q/dz , k-essence is hardly distinguishable from quintessence, unless $c_s^2 \approx 0$ since the surface of last scattering [26]. We will consider only canonical quintessence evolution with the Friedmann expansion rate (2).

II. ATTRACTORS IN BOTH TRACKING AND IN QUINTESSENCE-DOMINATED ERAS

The equations of motion enjoy a fixed attractor solution $\lambda = \text{const}$ (exponential potential), when $\beta = \infty$, and an *instantaneous attractor* solution [16, 17, 20, 23], when $\lambda\beta \gg 1$ makes λ slowly varying in equation (19) and the equation of state becomes [21]

$$\gamma_{Qatt}(\lambda) = \frac{1}{2}[(1+2/\beta)t + \gamma_B] - \sqrt{((1+2/\beta)t - \gamma_B)^2 + 8\gamma_B t/\beta} = \begin{cases} 0, & \beta = 0(\text{cosmological const}) \\ t - (1 - 2/\beta^2)t^2/2\gamma_B, & t \ll 1(\text{quintessence era}) \\ \gamma_B\beta/(\beta + 2), & t \gg 1(\text{background era}), \\ \gamma_B, & \beta = \infty(\text{exponential potential}). \end{cases}$$

where $t \equiv \lambda^2/3$. Defining $\Omega_{Qatt}(\lambda) = \gamma_{Qatt}/t$, $\lambda_{att} \equiv \sqrt{3\gamma_{Qatt}/\Omega_Q}$, so that $\Delta = \lambda/\lambda_{att} = \sqrt{\gamma_Q/\gamma_{Qatt}}$, the Attractor Condition is simply

$$\Delta \approx 1 \quad \text{or} \quad \lambda \approx \lambda_{att}. \quad (21)$$

Quintessence [16, 22, 23] exploits this attractor property to explain the very small present smooth energy density dynamically, without invoking a finely tuned cosmological constant.

We reserve the term *tracker* for attractors in the background-dominated era, for which β and $\gamma_Q = 2\gamma_B/(2+\beta)$ are nearly constant, so that $\Omega_{Qtr} \sim a^{3(\gamma_B - \gamma_Q)} \sim t^P$, where $P = 4/(2+\beta)$. *Good trackers* ($\beta > 1$, $\gamma_Q \lesssim \gamma_B$), have Ω_Q and λ_{att} slowly varying. Very good trackers ($\beta \gg 1$) approximate exponential potentials; because $\Omega_Q(z)$ was still appreciable in the distant past, they show *early quintessence*. In *poor trackers* ($\beta < 1$, $\gamma_Q \ll 1$), $\Omega_Q \sim t^2$, $\lambda_{att} \sim t^{-1}$ are changing with time and η can be appreciable, even when the roll λ is small.

Figure 1 shows the complete attractor phaseportraits, while tracking and while quintessence-dominated, for three forms of potential: constant w_Q (dashed), inverse power (solid), SUGRA (dotted), all chosen to reach $\Omega_{Q0} = 0.71$ at

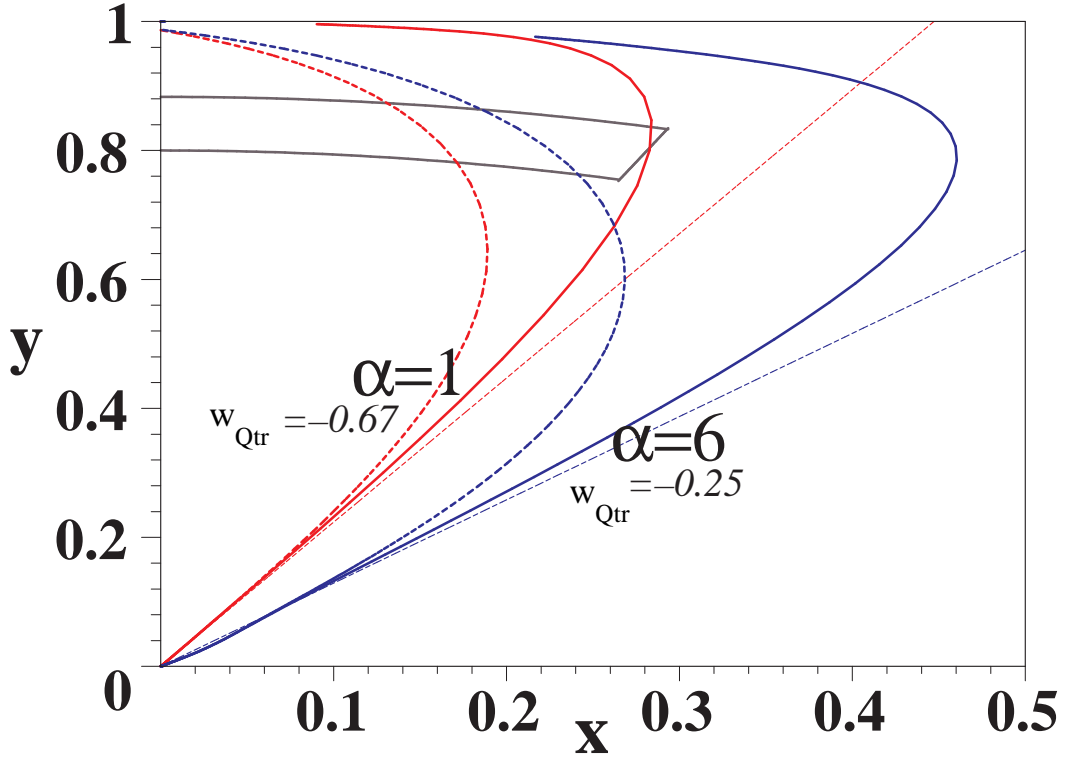


FIG. 1: Complete phase portraits of attractors now passing through $\Omega_{Q0} = 0.71$, for different curvature potentials: three steep potentials ($\alpha = 6, w_{Qtr} = -0.25$) on the right, three shallow potentials ($\alpha = 1, w_{Qtr} = -0.67$) on the left. In the background-dominated era $\Omega_Q = x^2 + y^2 \ll 1$, all attractors are nearly linear (track). At any Ω_Q , shallow potentials are poorer trackers than are steep potentials. In the quintessence-dominated era, different curvature effects emerge: both constant w_Q attractors (dashed) remain linear; both inverse power attractors (solid), start late to curve slowly towards the y-axis ($w_Q = -1$); both SUGRA attractors (dotted), start early to curve rapidly towards the y-axis. The trapezoidal region on the upper left is the observationally allowed present phase space.

TABLE II: Tracker and present ($\Omega_{Q0} = 0.71$) attractor solutions for inverse power potentials.

α	w_{Qtr}	$\log \Omega_{Qtri}$	M	w_{Q0}	x_0^2	y_0^2	η_0	λ_0	$\varkappa\phi_0$	$\log \Omega_{Qi}$ range
6	0..-0.25	-10.9	5.3 PeV	-0.41	.210	.499	2.69	1.519(fast)	3.949	-42..-0.5
1	-0.555..-0.667	-29.3	2.3 keV	-0.76	.083	.626	1.65	0.908	1.101	-41..-1.5
0.5	-0.733..-0.80	-35.2	4.8 eV	-0.86	.049	.661	1.42	0.689	0.73	-42.1..-9.1
0.1	-0.937..-0.952	-41.9	12.1 meV	-0.97	.011	.698	1.36	0.351(slow)	0.285	-42.2..-35.5
0	-1	-44.1	2.5 meV	-1	0	.71	0	0 (static)	-	-44.1

the present time. For each potential, the shallow potential $\alpha = 1$ attractor trajectories appear on the left, the steep $\alpha = 6$ attractor on the right. The cosmological constant trajectory $\alpha = 0$ is the y-axis. Not shown in the figure, is the exponential potential's fixed point, $x = \sqrt{\Omega_{Q0}/2} = y$, lying on the circle $\Omega_{Q0} = 0.71$. The presently observed trapezoidal region in phase space marginally allows the $\alpha = 1$ inverse power potential, but comfortably allows the SUGRA potential for a range in parameter α .

In the background dominated era, all these potentials track with phaseportrait slope $(y/x)_{tr} = \sqrt{V/K}$ gradually increasing from $\sqrt{1/2 + 3/\beta}$ in the radiation-dominated era to $\sqrt{1 + 4/\beta}$ in the matter-dominated era. Later, as quintessence begins dominating, this slope gradually steepens, so that the phase trajectories slowly approach the x-axis. At present, we are now past tracking but not yet de Sitter. For most potentials, $\phi_0 \sim M_P$, so that we need to consider trajectories whose present roll and curvature are $\mathcal{O}(1)$. After quintessence begins dominating, their different curvatures make these three potential forms evolve differently: the constant w_Q potential curves keep their tracker values, the SUGRA potential orbits curve strongly towards the y-axis (cosmological constant).

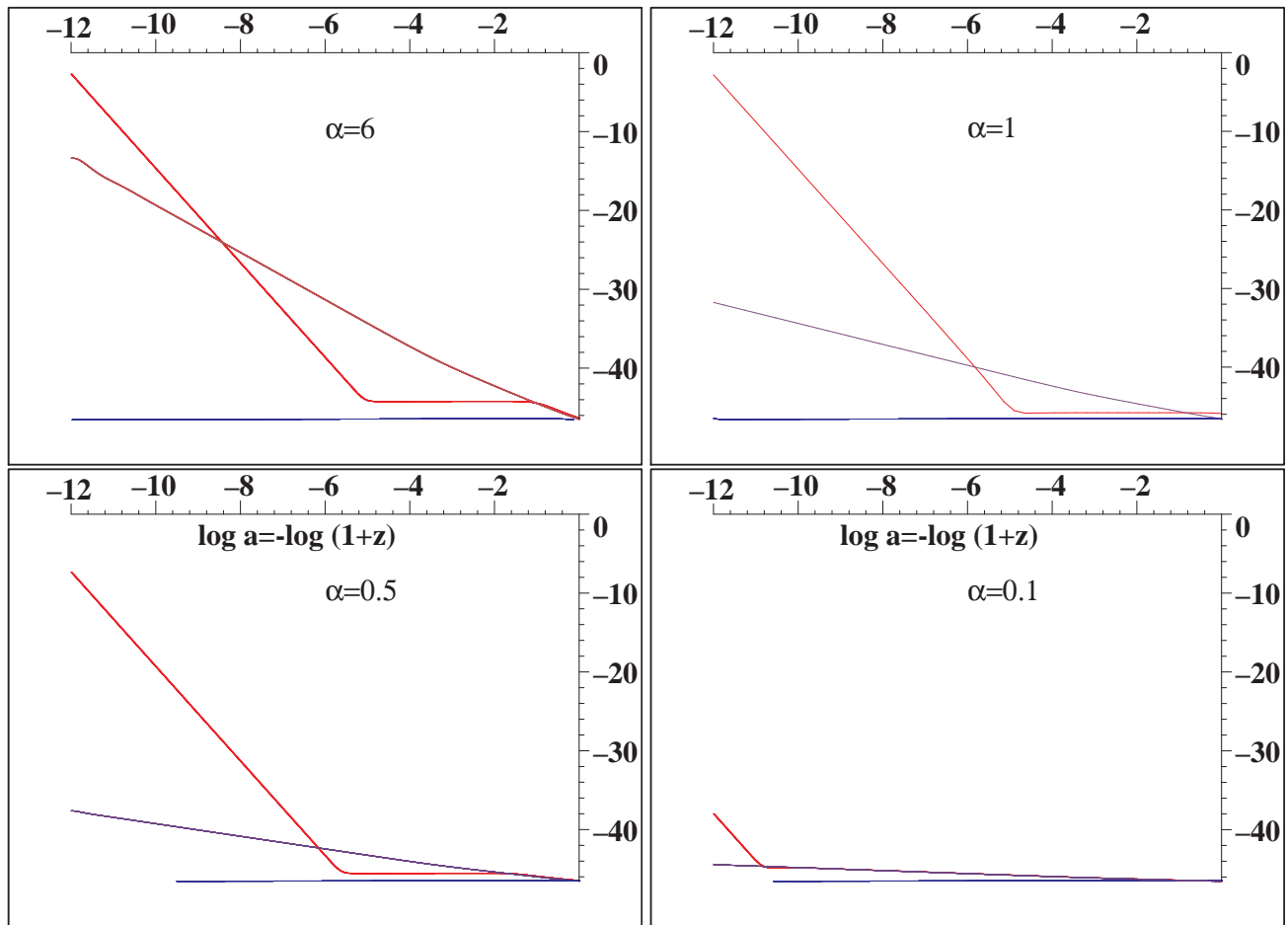


FIG. 2: Evolution of quintessence energy density, $\log \rho_Q (\text{GeV}^4)$ on vertical axes, for four inverse power potentials $\alpha = 6, 1, 0.5, 0.1$, from red-shift $z = 10^{12}$, to the present value $\rho_{Q0} = 0.71\rho_{cr0}$. In all figures, the central, trajectory is the attractor, starting with tracker slope $d \ln \rho_Q / dN = -6\gamma_B / (2 + \alpha)$. The lower curve is the maximal undershoot trajectory, which freezes immediately and then crawls slowly to join the attractor now. The upper curve is the maximal overshoot trajectory, which kinates with slope -6, before freezing late and now reaching the attractor. Poor trackers must freeze early, out of a narrow range in $\log \rho_{Qi}$.

III. SHALLOW INVERSE POWER POTENTIALS MAKE POOR TRACKERS

To obtain the presently small smooth energy without fine-tuning initial conditions, phase trajectories must flow onto the attractor before now and for a broad range of initial conditions, the *basin of attraction*. A good tracker starts from a broad basin of attraction and freezes with $w_Q \sim -1$, before tracking with kinetic energy/potential energy ~ 1 . A poor tracker starts from a narrow basin of attraction and freezes for a long time, before tracking with kinetic energy/potential energy $\ll 1$.

In poor attractors, this shrinkage of the basin of attraction, making the present universe sensitive to initial conditions, derives from early freezing. From any *undershoot* initial conditions $\rho_{Q0} < \rho_{Qi} < \rho_{Qtr}$, freezing emerges directly. (Indeed, if the initial density ρ_{Qi} is small enough, the field crawls down to its present value ρ_{Q0} , without ever tracking.) But, starting from *overshoot* initial conditions $1 > \Omega_{Qi} > \Omega_{Qtr}$, freezing starts much later, at a value $\phi_{fr} \gtrsim M_P \sqrt{6\Omega_{Qi}}$, only after a long kinated era ($x \gg y$), during which $\dot{\phi}^2 \approx 2\rho_Q$ lets the field grow rapidly while Ω_Q decreases. Too much overshoot would make the phase trajectories freeze so late as to reach the attractor only in the future.

We must now extend earlier treatments [16, 17] of trackers to solutions that reach the attractor only now, in the present, quintessence-dominated era. When the curvature is large, tracking will stop early, while $\lambda \sim \beta$ is already slow-rolling. Attractors that only now become approximately slow-rolling ($\lambda_0 < 1$) could only have been reached from a narrow tracking basin of attraction. Indeed, in the static limit (cosmological constant), the present smooth energy arises out of the unique initial condition $\rho_{Qi} = \rho_{Q0}$.

TABLE III: Quintessence potentials which track early, but crawl now.

Potential $V(\phi)$	Theoretical Origin	References
$M^4[\cos(\phi/f) + 1]$	String, M-theory pseudo Nambu-Goldstone light axion	[14, 36, 39, 40]
$M^{4+\alpha}\phi^{-\alpha} \cdot \exp \frac{1}{2}(\kappa\phi)^\beta/2$	SUGRA, minimum at $(\kappa\phi)^\beta = 2\alpha/\beta$	[27, 28, 29]
$M_P^4[A + (\kappa\phi - \kappa\phi_m)^\alpha] \exp(-\lambda\kappa\phi)$	Exponential modified by prefactor, to give local minimum; M-theory	[41, 42]

For the simple inverse power law potentials

$$V(\phi) = M_\alpha^{4+\alpha}/\phi^\alpha, \quad (22)$$

the curvature $\beta = \alpha = \text{constant}$, so that the equation of motion (10) has exactly scaling solutions in both the radiation- and the matter-dominated eras. These potentials are interesting, because they approximate any potential, while tracking. They arise naturally in supersymmetric condensate models for QCD or instanton SUSY-breaking [27, 28, 29], but acquire appreciable quantum corrections when $\phi \gtrsim M_P$. For these potentials, $\lambda \sim V^{1/\alpha} \sim (yH)^{2/\alpha}$, the third equation (19) integrates to $\lambda = \lambda_0(yH/y_0H_0)^{2/\alpha}$ in terms of present values of y , H , λ .

The second column in Table II gives the range in tracker values w_{Qtr} , from $(\alpha - 6)/3(\alpha + 2)$, during the radiation-dominated era, to $-2/(\alpha + 2)$, during the matter-dominated era. The third column gives the initial Ω_{Qtri} values at $z = 10^{12}$ a tracker must have in order to reach the present value $\Omega_{Q0} = 0.71$. The fourth column tabulates the quintessence energy scales needed, in order to reach $\Omega_{Q0} = 0.71$.

After tracking, these trajectories curve towards the $x = 0$ (asymptotic de Sitter) axis. Between the two vertical double bars, columns five through ten, summarize the present (post-tracker) values for trajectories that have tracked before now. The steep $\alpha = 6$ trajectory would by now track down only to $w_{Q0} = -0.41$, which is excluded observationally by the constraint (8), which requires $\alpha \lesssim 1$ [16].

Integrating equations (17,18) shows, in the last column, for each α , the range of initial Ω_{Qi} that would track and finally reach the presently-allowed value $\Omega_{Q0} = 0.71$. For large α , the quintessence potential would now still be fast-rolling [4]. As α decreases, w_{Q0} decreases, but the basin of attraction shrinks. For $\alpha < 0.5$, the presently-tracking range in initial values of $\log \Omega_{Qi}$ is already 9 orders of magnitude narrower than the initial range of the good $\alpha = 6$ trackers first considered [16]. For a cosmological constant ($\alpha = 0$), the present value is realized only if it is initially tuned uniquely to its present value $\rho_Q = 28.8 \text{ meV}^4$.

Because the observed \widetilde{w}_Q is already close to the cosmological constant value -1 , an inverse power potential requires $\alpha < 1$, so that the potential energy *always* dominated the kinetic energy ($x \ll y$). These nearly flat trajectories never track, but "crawl" [30] towards their present values, only because they were initially tuned close to these values. For a good tracker to nevertheless reach $\widetilde{w}_Q < -0.78$, its post-tracker potential needs $\beta(\phi)$ decreasing, $P(\phi)$ increasing, so that $\Omega_Q \sim t^P$ grows rapidly at late times [16]. Such *cross-over quintessence* [13] is characterized by $w_Q(z)$ reduction in the recent past ($z < 0.5$).

IV. ONCE GOOD TRACKERS NOW ROLLOVER TOWARDS LARGE POTENTIAL CURVATURE

We have not considered models with a true cosmological constant, matter-coupled quintessence, quantum corrections to classical quintessence, k-essence [24, 26], nor large extra dimension or brane models [37, 38], for which the Friedmann equation is modified at very early times. But, within canonical quintessence, the observations allow phase trajectories that are insensitive to initial conditions, only if the curvature increases rapidly near the present epoch $\kappa\phi_0 \sim 1$, so that quintessence-domination and kinetic energy suppression began only recently.

This needed post-tracking behavior is illustrated in the popular potentials listed in Table III. (A longer list of potentials is given in references [31, 32, 33, 34].) For example, the SUGRA models on the last line of Table I have minima at $\kappa\phi = \sqrt{\alpha}$. The dotted curves in Figure 1 show that far below this minimum, they behave and track like inverse power potentials, but near the minimum, the curvature increases rapidly. After tracking in the background-dominated era, these SUGRA phase trajectories, for $\alpha = 6$ and 1, both curve over to lower w_{Q0} values, in marginal agreement with observations, for a large range in α values.

A good tracker, insensitive to initial conditions, requires a rapidly changing potential curvature, making $\widetilde{w}_Q(z)$ fast-changing only recently, at red-shifts $z \lesssim 0.5$. Difficult combined supernova, CBR and cosmic shear observations in the next decades may yet distinguish quintessence from a true cosmological constant [31, 35]. Otherwise, quintessence appears hardly distinguishable, theoretically and phenomenologically, from the small cosmological constant it was designed to explain.

The original cosmological coincidence problem was to understand why the smooth energy density is *now* so small, fortunately allowing large scale structure formation, before lately dominating the matter energy density. By requiring that the smooth energy density now be small *and* fast-changing, this coincidence problem is now exacerbated. In two ways. recent cosmological observations stress the special time in which we live, which may call for anthropic reasoning in cosmology.

Acknowledgments

We are indebted to Martin Block for help with the numerical integration of the scalar field dynamical equations and to US Department of Energy grant DE-FGO2-95ER40893 at the University of Pennsylvania for partial travel support.

-
- [1] I. Moar, R. Brustein, J. McMahon and P. J. Steinhardt, Phys. Rev. **D65** 2002, 12303.
 - [2] T. Nakamura and T. Chiba, Mon. Not. R. Astron. Soc. **306** (1999), 696.
 - [3] D. Huterer and M. S. Turner, Phys. Rev. **D60** (1999), 081301; Phys. Rev. **D64**(2001).
 - [4] S. Bludman and M. Roos, Astrophys. J. **547** (2001), 77.
 - [5] D. N. Spergel *et al.*, submitted to Astro. Ph. (2003).
 - [6] J. L. Tonry *et al.*, arXiv:astro-ph/0305008 (2003).
 - [7] R. Bean and A. Melchiorri, Phys. Rev. **D65** (2002), 041302-1.
 - [8] P. S. Corasaniti and E. J. Copeland, Phys. Rev. **D65** (2002), 043004-1.
 - [9] G. Efstathiou *et al.*, Mon. Not. R. Astron. Soc. **330** (2002), L29.
 - [10] M. Tegmark, Science **296** (2002), 467.
 - [11] X. Wang, M. Tegmark and M. Zaldarriaga, Phys. Rev. **D65** (2002), 123001.
 - [12] J. Richard Bond *et al.*, arXiv:astro-ph/021007 (2002).
 - [13] R. R. Caldwell, M. Doran, C. M. Mller, G. Schfer and C. Wetterich, arXiv:astro-ph/0302505 v1 (2003).
 - [14] R. R. Caldwell, R. Dave and P. J. Steinhardt, Phys. Rev. Lett. **80** (1998), 1582.
 - [15] C. Wetterich, arXiv:hep-ph/0301261 v1 (2003).
 - [16] P. J. Steinhardt, L. Wang and I. Zlatev, Phys. Rev. **D59** 1999, 123504.
 - [17] I. Zlatev, L. Wang and P. J. Steinhardt, Phys. Rev. Lett. **82** (1999), 890.
 - [18] P. Ferreira and M. Joyce, Phys. Rev. Lett. **79** (1997), 4740; Phys. Rev. **D57** (1998), 6022.
 - [19] A. R. Liddle and J. Scherer, Phys. Rev. **D59** 1998, 02359.
 - [20] E. J. Copeland, A. Liddle and D. Wands, Phys. Rev. **D57** 2001, 4686.
 - [21] S. C. C. Ng, N. J. Nunes and F. Rosati, Phys. Rev. **D64** 2001, 083510.
 - [22] B. Ratra and P. J. E. Peebles, Phys. Rev. **D37** (1988), 3406.
 - [23] C. Wetterich, Nucl. Phys. **B302** (1988), 668.
 - [24] C. Armendariz-Picon, V. Mukhanov and P. J. Steinhardt, Phys. Rev. Lett. 2000, 4438; Phys. Rev. **D63** (2001), 103510.
 - [25] J. K. Erikson, R. R. Caldwell, P. J. Steinhardt, C. Armendariz-Picon and V. Mukhanov, Phys. Rev. Lett. **88** (2002), 121301.
 - [26] V. Barger and D. Marfata, Phys. Lett **B498** (2001), 67.
 - [27] P. Binutray, Phys. Rev. **D60** (1999), 063502.
 - [28] Ph. Brax and J. Martin, Phys. Lett **B468** (1999), 40.
 - [29] Ph. Brax, J. Martin and A. Riazuelo, arXiv:hep-th/0109207 (2001).
 - [30] G. Huey and J. E. Lidsey, Phys. Lett **B514** (2001), 217.
 - [31] J. Weller and A. Albrecht, Phys. Rev. **D65** (2002), 103512.
 - [32] V. Sahni, Chaos **16** (2003) 527.
 - [33] P. J. E. Peebles and B. Ratra, arXiv:astro-ph/0207347 (2002).
 - [34] V. Sahni and A. Starobinski, Int. J. Mod. Phys. **D9** (2000) 373.
 - [35] J. A. Frieman, D. Huterer, E. V. Linder and M. S. Turner, arXiv:astro-ph/0208100 (2002).
 - [36] K. Choi, Phys. Rev. **D62** (2000), 043509.
 - [37] N. J. Nunes and E. J. Copeland, arXiv:astro-ph/0204115 (2002).
 - [38] A. Albrecht, C. P. Burgess, F. Ravndal and C. Skordis, Phys. Rev. **D65**(2002), 123507.
 - [39] J. Frieman, C. T. Hill, A. Stebbins and T. Waga, Phys. Rev. Lett. **75** (1995), 2077.
 - [40] K. Coble, S. Dodelson and J. A. Frieman, Phys. Rev. **D55** (1997), 1851.
 - [41] A. Albrecht and C. Skordis, Phys. Rev. Lett. **84** (2000), 2076.
 - [42] C. Skordis and A. Albrecht, Phys. Rev. **D66** (2002), 043523.